Aptamers

ISSN 2514-3247 | OPEN-ACCESS | PEER-REVIEWED

RESEARCH ARTICLE

Preliminary *in vivo* characterization of a theranostic aptamer: Sgc8-c-DOTA-^{67}Ga

Victoria Calzada[1*], Jessica Báez [1], Estefanía Sicco[1], Jimena Margenat[1], Marcelo Fernández[2], María Moreno[3], Manuel Ibarra[4], Thomas Quinn[5], Juan Pablo Gambini[6], Pablo Cabral[1] and Hugo Cerecetto[1]

[1]Área de Radiofarmacia, Centro de Investigaciones Nucleares, Facultad de Ciencias, Universidad de la República, Uruguay; [2]Laboratorio de Experimentación Animal, Centro de Investigaciones Nucleares, Facultad de Ciencias, Universidad de la República, Uruguay; [3]Departamento de Desarrollo Biotecnológico-Instituto de Higiene, Facultad de Medicina, Universidad de la República, Montevideo, Uruguay; [4]Centro de Evaluación de Biodisponibilidad y Bioequivalencia de Medicamentos, Universidad de la República, Montevideo, Uruguay; [5]Department of Biochemistry, University of Missouri, Columbia, MO USA; [6]Centro de Medicina Nuclear, Hospital de Clínicas, Facultad de Medicina, Universidad de la República, Uruguay

*Correspondence to: Victoria Calzada, Email: vcalzada@cin.edu.uy, Tel: +589 98444402

Received: 22 June 2017 | **Revised:** 14 December 2017 | **Accepted:** 15 December 2017 | **Published:** 15 December 2017

© Copyright The Author(s). This is an open access article, published under the terms of the Creative Commons Attribution Non-Commercial License (http://creativecommons.org/licenses/by-nc/4.0). This license permits non-commercial use, distribution and reproduction of this article, provided the original work is appropriately acknowledged, with correct citation details.

ABSTRACT

Nucleic acid aptamers can recognise their target with high affinity and specificity, and their potential as molecular imaging agents and use in theranostics are being explored. Compared with antibodies, aptamers can be easily synthesized and chemically modified, rendering them a valuable tool for *in vivo* approaches. Herein, we investigated a 41nt DNA aptamer as a theranostic agent for lymphoma and melanoma. This aptamer exhibits specific binding and high affinity for the PTK7 receptor that is overexpressed in many cancer cells. A 5'-amino-derivative of the Sgc8-c aptamer was bound to the metal chelator DOTA (1,4,7,10-tetraazacyclododecane-1,4,7,10-tetraacetic acid) and labelled with the radionuclide ^{67}Ga, forming the aptamer probe Sgc8-c-DOTA-^{67}Ga. Different conditions during synthesis, purification and identification of the intermediate and final radiolabelled probe, were examined. Aptamer modification and radiolabelling were performed with high yields, resulting in a probe that was stable in neutral buffered solution. Binding to PTK7 was studied in CCRF-CEM, A20 and B16F1 cell lines, and in purified PTK7-1 receptor, to confirm specificity. The *in vitro* cell lines showed different levels of uptake, and the signal increased over time. *In vivo* binding properties were studied in A20 and B16F10 tumour-bearing mice and images were acquired using X-rays and gamma imaging modalities for both models. Preliminary results in both tumour models showed good aptamer uptake by tumour. Hepatobiliar metabolism was observed with Sgc8-c-DOTA-^{67}Ga and no signal was detected in normal tissue. In summary, these results support the utility of labelled aptamers as theranostic agents in different imaging modalities and theranostic.

KEYWORDS: Aptamer, Sgc8-c, PTK7, molecular imaging, theranostic.

INTRODUCTION

Since first reported (Ellington and Szostak, 1990; Tuerk and Gold, 1990), the use of aptamers has principally focused on biochemical and enzymatic applications. However, in recent years several aptamers have been developed for biomedical applications including molecular imaging, diagnostics, therapeutics and drug delivery (Röthlisberger etal, 2017; Garcia-Recio etal, 2016; Cao et al, 2014; Sun et al, 2014).

Aptamers are oligonucleotides (DNA or RNA) that are selected to specifically recognise a molecular target with high affinity. The selection process is carried out using an iterative procedure known as Systematic Evolution of Ligands by Exponential Enrichment (SELEX) (Osborne and Ellington, 1997; Breaker, 2004; Wu and Kwon, 2016; Darmostuk, 2015). Aptamers are considered “rivals” to antibodies for their ability to recognize bio-target (Jayasena, 1999). Aptamers offer several advantages. Firstly, they can be easily synthesised, resulting in a reliable, scalable and economic process. Secondly, oligonucleotides are temperature- and pH-stable, and a variety of post-SELEX chemical modifications can be introduced to confer desirable characteristics (Gao et al, 2016). Furthermore, aptamers have a low molecular weight (~15000Da), allowing fast tissue penetration and body clearance and animal studies have shown that they are non-immunogenic (Borbas et al, 2007; Hwang do, 2010).

These favourable characteristics have encouraged the development of aptamers for clinical application (Nozari and Berezovski, 2016; Stein and Castanotto 2017). The FDA has approved aptamers for use as therapeutic agents and several clinical trials are currently underway (Kanwar et al, 2015; Parashar, 2016).

The use of aptamers as molecular imaging agents has been reported in a number of previous studies (Charlton et al, 1997; Lee and Li, 2011; Wang and Farokhzad 2014). These studies provide a better understanding of the *in vivo* patterns of molecular diversity in cancer and contribute to conventional imaging techniques (Weissleder and Mahamood, 2001; Histed et al, 2012; Palestro, 2014). Aptamer-based theranostic strategies are part of this development and allow simultaneous imaging guide and targeted therapy using the same probe basis (Drude et al, 2017). Theranostics are a combination of diagnostics and therapy and allow personalised management of disease

(Baum et al, 2012). As a result, there has been an enormous increase in *in vivo* aptamer applications, but challenges still remain.

Shangguang and co-workers identified the original Sgc8 sequence, selected from a 10^{15} ssDNA aptamer library, to target acute lymphoblastic leukaemia T cells (Shangguan et al, 2007; Shangguan et al, 2008; Jacobson et al, 2015). Here, we studied Sgc8-c, which is a truncated version of the Sgc8 DNA aptamer, containing only 41 nt. Sgc8-c has an affinity of 0.78nM against the PTK7 receptor, which was originally reported to be overexpressed in colon cancer and later-identified in haematological tumours and other malignancies (Berger et al, 2017; Xiao et al, 2008).

We previously evaluated a few derivatives of the DNA aptamer Sgc8-c aptamer as molecular imaging agents and theranostics (Calzada et al, 2017; Sicco et al, 2017). In this study, we evaluated the Sgc8-c 5'-amino derivative, conjugated with DOTA, which was radiolabelled with ^{67}Ga as a theranostic agent. Sgc8-c is a 41nt DNA aptamer against the PTK7 receptor (Shangguan et al, 2006; Shangguan, 2007).

The metal chelator 1,4,7,10-tetraazacyclododecane-1,4,7,10-tetraacetic acid (DOTA), is able to coordinate to metal ions such as Ga^{3+}, Zr^{4+}, Cu^{2+}, In^{3+}, Lu^{3+}, Y^{3+} and Bi^{3+} (Calzada et al, 2012; Sicco et al, 2017), and therefore, we explored the potential use of radiolabelled Sgc8-c-DOTA as a possible theranostic agent in cancers. Herein, chemical synthesis and purification techniques for preparing radiolabelled Sgc8-c-DOTA-^{67}Ga aptamer were optimised. This was followed by receptor binding assays and *in vivo* pharmacokinetic and tumour targeting studies to validate the aptamer's potential as a theranostic agent.

MATERIALS AND METHODS

Aptamer conjugation (Sgc8-c-DOTA)

The 5'-(6-aminohexyl)-modified Sgc8-c aptamer (13 kDa, 5'- /6-AM/ATC TAA CTG CTG CGC CGC CGG GAA AAT ACT GTA CGG TTA GA -3', Sgc8-c-NH_2) (Calzada et al, 2017; Sicco et al, 2017) was purchased from IDT technologies (Integrated DNA Technologies, Inc. IA, USA) . 1,4,7,10-tetraazacyclododecane-1,4,7,10-tetraacetic acid mono-*N*-hydroxysuccinimide ester as $HPF_6.CF_3CO_2H$ salt (NHS-DOTA, B-280, Macrocyclics, Inc. TX, USA, 0.76 mg, 1 µmol) dissolved in dry

DMSO (3.85 µl) was added to a solution of Sgc8-c-NH_2 (0.13mg, 0.01µmol) with a mixture containing equal volumes of sodium phosphate buffer (0.1M, pH=8.5) and sodium bicarbonate (0.1M, pH=8.5) (total volume of the mixture of 400µl). The reaction mixture was stirred in the dark at room temperature for 2hr. The reaction was stopped by buffer exchange using Microcon® Centrifugal Filters (10 kDa cut-off) or PD10 column chromatography (GE Healthcare Life Sciences, Little Chalfont, UK) with MilliQ water and detection by spectrophotometry at 260 nm. Progress of the reaction and quality of the product were monitored using Reverse-Phase High Performance Liquid Chromatography (RP-HPLC) (Agilent 1200 Series Infinity Star, Santa Clara, USA) with a 5µm C-18 Kinetex column (Phenomenex) run with an aqueous solution of triethylamine (50mM, pH=7.5)/5% ,v/v, acetonitrile (solvent A) and methanol (solvent B), at a flow rate of 1ml/min and a gradient of A:B (90:10) to A:B (40:60) over 30min (UV detection). In addition, gel electrophoresis (native polyacrylamide, 15%, w/v) was performed.

The conjugation yield was 77% by RP-HPLC and the conjugated was confirmed by ESI-MS (IDT technologies). Molecular weight of the conjugated was in 13238.5Da (with coordinated potassium); expected: 13238.5Da (with coordinated potassium). After purification, fractions were dissolved in MilliQ water or lyophilised and stored at 4°C and -20°C and stability was measured over the time.

Sgc8-c-DOTA radiolabelled

The lyophilized aptamer Sgc8-c-DOTA (20 µg, 0.0015 µmol) was dissolved in ammonium acetate buffer (0.1M, pH =5.0) (300µl) and 10MBq of an aqueous solution of $^{67}GaCl_3$ (Tecnonuclear, Buenos Aires, Argentina) was added. The mixture was adjustment to a final volume of 1ml and pH =5.0 incubated at 60°C for 30min.

The radiolabelling yield and radiochemical purity of the product were monitored using RP-HPLC as described above using gamma detection.

Physicochemical characterization

Sgc8-c-DOTA-^{67}Ga was incubated with 500µl fetal bovine serum (FBS) for 24h at 37°C. The mixture was filtered (0.22µm) and stability controls were performed using a normal-phase HPLC system in a size exclusion column with a pore size of 300A, 7.5x300mm (Waters), a phosphate buffer 0.01M,

a flow rate 1ml/min over 20min. The same procedure and conditions were used with a saline solution (NaCl 0.9%).

The partition coefficient (LogP) was calculated for Sgc8-c-DOTA-^{67}Ga by incubating with an *n*-octanol and phosphate-buffered saline (PBS) (1:1) mixture. The mixture was vortexed for 1min and centrifuged for 5min at 1000x*g*. Aliquots of each phase were measured, in triplicate, in a gamma counter.

Binding experiments

A maximum binding capacity assay was performed according to the Lindmo method (Lindmo et al, 1986). Different amounts of PTK7-1 (TP700163, Origene, MD, USA) were adsorbed in Nunc tubes (Brandt®) and serial dilutions of the receptor were prepared in 2ml PBS to give final concentrations of 0.78, 0.39, 0.049, 0.024, 0.012, 0.0061 and 0.0030nM. Samples were prepared in triplicate. After incubation for 24hr at room temperature with continuous orbital shaking, tubes were washed three times with PBS. Finally, 100000cpm of radiolabelled aptamer, Sgc8-c-DOTA-^{67}Ga, were incubated 1hr at room temperature. Tubes were washed three times with PBS and the radioactivity was quantified using a gamma counter. The non-specific binding was determinated by incubating with FBS.

Sgc8-c-DOTA-^{67}Ga cell binding was studied in B16F1 mouse melanoma and A20 mouse B-cell lymphoma cell lines, both from ATCC (American Type Culture Collection, VA, USA). The human acute lymphoblastic leukaemia cell line CCRF-CEM (ATCC) was used as a positive control in this study (Shangguang et al, 2008). B16F1 cells were grown in Dulbecco's Modified Eagle's Medium (DMEM) (PAA Laboratories Ply Ltd, Australia) supplemented with 10% (v/v) FBS and 2mM L-glutamine (Sigma-Aldrich, St. Louis, USA). A20 cells were grown in a suspension of RPMI-1640 medium (Sigma-Aldrich, St. Louis, USA) supplemented with 10% (v/v) FBS, 2mM L-glutamine and 0.05mM β-mercaptoethanol (Sigma-Aldrich, St. Louis, USA). CCRF-CEM cells (ATCC) were grown in RPMI-1640 medium supplemented with 10% (v/v) FBS and 2mM L-glutamine. All cell lines were cultured at 37^{o}C with 5% (v/v) CO_2. Adherent B16F1 cells were surface detached using a cell scraper.

All cells were then washed twice by gentle centrifugation with sterile PBS (pH=7.4) and $1.0x10^6$ cells were re-suspended in a final volume of 1ml PBS and incubated with 100000cpm of Sgc8-c-DOTA-^{67}Ga. The probe was incubated for 0.5, 1, 2 and 4hr at 37°C. Cells were washed twice with PBS and radioactivity in the pellets was quantified as described above. The tubes were measured in a gamma counter.

A competition binding assay was performed with positive CCRF-CEM cell line to confirm the specificity of the radiolabelled aptamer. A 100nM excess of the non-radiolabelled aptamer (Sgc8-c-NH_2) was incubated for 30min at 37°C to block Sgc8-c-DOTA-^{67}Ga specific binding. After incubation with Sgc8-c-NH_2, cells were washed with PBS and incubated with 100000 cpm of Sgc8-c-DOTA-^{67}Ga. The probe was incubated for 2hr at 37°C. Cells were washed twice with PBS and radioactivity in the pellets was quantified as described above.

Biodistribution and pharmacokinetics

Biodistribution of Sgc8-c-DOTA-^{67}Ga was assayed in normal BALB/c mice with 20–25gm bodyweight (provided by the Laboratorio de Experimentación Animal, Centro de Investigaciones Nucleares (LEA-CIN, Montevideo, Uruguay). Approximately 1850kBq radiolabelled aptamer was intravenously (IV) administered via the tail vein. At 0.5, 2, 4 and 24hr after aptamer administration, mice (n=5 per time) were sacrificed by cervical dislocation and organs were weighed and measured in a gamma counter. Radioactivity levels in each tissue were expressed as percentages of injected dose per gram of tissue (%ID/g) and as percentages of injected dose (%ID).

The pharmacokinetic profile was assessed by bolus IV administration of individual doses of 5.5–9.2MBq Sgc8-c-DOTA-^{67}Ga into the tail vein of Wistar® rats with 200–250gm bodyweight (purchased from DILAVE, Montevideo, Uruguay). Blood samples were collected in a capillary tube from the ocular globe at 0.25, 0.5, 1, 2, 4, 18, 24 and 48hr (n=3 per time) following aptamer administration. Samples were weighed and radioactivity was measured in a gamma counter. Urine was also collected over a 48hr period to assess renal elimination. A compartmental pharmacokinetic analysis was performed and the akaike information criteria (AIC) value was compared for each model. The parameters as volume of distribution at steady state (Vss) and clearance (CL) were calculated.

Tumour uptake experiments

Imaging studies were performed in two tumour-bearing mice models. Female C57BL/6 and BALB/c mice (from LEA-CIN, Montevideo, Uruguay), 6–8 weeks old with 20–25gm body weight, were used for *in vivo* experiments. For tumour implantation, C57BL/6 and BALB/c mice were inoculated subcutaneously with $2.5x10^5$ B16F1 and $1.0x10^6$ A20 cells, respectively (n=3) (Calzada et al, 2017). When tumours were palpable, on approximately day 10 and day 20, respectively, Sgc8-c-DOTA-^{67}Ga was administered by bolus IV injection. After 2 and 24hr, mice were anaesthetised with isoflurane. Images for both mice models were taken in an In-Vivo MS FX PRO instrument (Bruker, Billerica, USA), using X-ray and gamma modes (10min acquisition). After each imaging time point, mice were sacrificed for organ dissection, and imaged and counted separately using the imaging equipment and gamma counter. Organ weight correction was applied and tumour/blood and tumour/muscle ratios were calculated.

All protocols for animal experimentation were carried out in accordance with procedures authorized by the University's Ethical Committee for Animal Experimentation, Uruguay, to whom this project was previously submitted. Animals were kept with water and food *ad libitum*.

RESULTS

Conjugation, radiolabel and physicochemical characterization

Preparation of the Sgc8-c-DOTA conjugate was optimized. The following variables were studied to optimise the procedures: i) reactants molar ratios; ii) time; and iii) reaction buffer (Sicco et al, 2017). Under the best conditions, Sgc8-c-NH_2 was reacted with NHS-DOTA to yield the desired conjugate with high purity.

Gentle reaction conditions resulted in fast DOTA conjugation and easy purification (Figure 1). Significant differences in reaction yield were observed depending on the buffer solutions with a 77% derivatisation yield from a mixture with equal volumes of Na_3PO_4 (0.1M) and $NaHCO_3$ (0.1 M) buffers (pH= 8.5) and 2hr reaction time. No improvement in product yield was observed with reaction times over 24hr. The optimal ratio of Sgc8-c-NH_2:NHS-DOTA was determined as 1:200. The RP-HPLC chromatogram of the crude reaction is shown in Figure 2 (top). Unreacted DOTA-NHS eluted first, followed by two peaks at 10.8min and 11.5min that were isolated and analysed. ESI-

MS analysis revealed that the first peak corresponded to Sgc8-c-NH_2 with an $M^{+\cdot}$ of 12812.5Da and the second peak to Sgc8-c-DOTA with $M^{+\cdot}$ of 13238.5Da.

Sgc8-c-DOTA samples were stored for over a month under different temperature conditions. Subsequent analysis by RP-HPLC showed that there were no significant changes in stability of the samples.

Different Sgc8-c-DOTA ^{67}Ga-radiolabelling times and temperatures (25, 37, 45, 60 and 75^{o}C) were assayed. The best optimum conditions for radiolabelling were in the presence of $^{67}GaCl_3$ at pH 5.0 and a temperature of 60^{o}C for 30min (Figure 1). According to RP-HPLC analysis (Figure 2) Sgc8-c-DOTA-^{67}Ga had up to 95% purity with a maximum specific activity of 450MBq/mg.

HPLC analysis demonstrated that Sgc8-c-DOTA-^{67}Ga was stable in an aqueous physiological solution for over 24h at 37^{o}C. Stability in FBS at 37^{o}C exhibited a half-life of 2hr (data not shown). Sgc8-c-DOTA-^{67}Ga exhibited a LogP value of -1.87±0.05, showing that the probe's hydrophilic characteristics were maintained after chemical modifications, as previously observed for other Sgc8-c-probes (Calzada et al, 2017).

Binding experiments

The immunoreactivity of Sgc8-c-DOTA-^{67}Ga was evaluated using a purified recombinant human PTK7 protein expressed in HEK293 cells. Binding results were depicted as binding fraction / total (B/T, Figure 3) of the incubated probe versus PTK7-1 concentration. A saturation profile was observed with a K_d of 11.4±0.1µM for Sgc8-c-DOTA-^{67}Ga. Binding studies on tumour cell lines were performed based on previous results (Calzada et al, 2017). A signal increase was observed over time for all A20, B16F1 and CCRF-CEM tumour cell lines. Moreover, all cell lines showed similar binding to Sgc8-c-DOTA-^{67}Ga. On blocking the CCRF-CEM cell line with the cold aptamer (Sgc8-c-NH_2) a 60% decrease in signal was observed (data not shown).

Biodistribution in normal mice

The biodistribution of Sgc8-c-DOTA-^{67}Ga in healthy animals is shown in Table 1. Low blood values were observed at all assayed time points. After 30min post injection, a value of 12.99±0.94 %ID/g was observed, which decreased over time to 3.55±1.79 %ID/g at 24hr. On the other hand, there

were no significant changes in liver activity over time (13.19±3.10%ID/g at 24hr post-injection). Kidney activity slightly increased over time (8.65±1.38%ID/g at 24hr) with concomital increase in urine and bladder activity of 31.23±1.90%ID. There was no significant uptake in non-target organs.

Pharmacokinetic study

The pharmacokinetic profile in rats showed that the behaviour of Sgc8-c-DOTA-^{67}Ga was consistent with a two-compartment pharmacokinetic model, with first-order kinetics for both distribution and elimination from the central compartment. The derived parameters indicated a fast distribution, since the half-lives of the initial and terminal disposition phases 0.678±0.23hr and 12.32±6.43hr, respectively. Mean residence time in the blood was 14.91±7.48hr. The Vss and blood clearance were 42.18±8.68l/kg and 2.72±1.31ml/min/kg, respectively, showing a large distribution and elimination that are lower than the average glomerular filtration rate. Renal clearance (CLr) was variable between rats (0.51±0.06ml/min/kg).

Imaging and tumour uptake

Planar gamma images were taken after IV injection of Sgc8-c-DOTA-^{67}Ga. X-rays and gamma images are shown in Figures 4 and 5 for B16F1 and A20 mouse models at 2hr post- aptamer injection. Unexpected abdominal activity was observed at 2 and 24hr post injection. A slight asymmetry in the tumour area was observed at both time points indicating tumour uptake.
In order to confirm the tumour uptake at 24hr, these results were corroborated by *ex vivo* imaging. Following *in vivo* imaging, mice were sacrificed and selected organs and tissue were examined using the same imaging methodology (Figure 6). *Ex vivo* imaging of the melanoma model showed a clear signal in the tumour, with a high signal in the liver and lower signal in the intestines. Low levels of radioactivity were observed in all other non-target organs. E*x vivo* imaging of the lymphoma model showed a low signal in the tumour, with high signals in the liver and lower signal in the intestines followed by the kidneys. The strong signal in the liver masked the rest of the organs. Values were quantified in a gamma counter and a weight correlation was applied. At 24hr post injection, tumour / blood and tumour / muscle activity ratios for both models were 6.5 and 9.0, respectively, for B16F1-tumour- bearing mice and 18.5 and 15.0, respectively, for A20-tumour- bearing mice.

DISCUSSION

Aptamers are promising molecular probes for cancer diagnosis and therapy (Cao et al, 2014). Sharing characteristics of peptides and antibodies, aptamers have advantages due to their easy synthesis, facile chemical modification and low immunogenic potential (Hicke et al, 2006; Borbas et al, 2007; Shangguan et al, 2008; Da Pieve et al, 2009; Lee and Li 2011). These biomolecules can be modified to functionalised probes for *in vivo* diagnostic and therapeutic purposes. Moreover, aptamers have properties that make them ideal as theranostics. Their Low molecular weight, fast tissue penetration and clearance, result in high target/non-target ratios (Hwang do et al, 2010). Therefore, theranostics could include aptamers as molecular probes. Theranostics allow visualisation and treatment in the same probe. Imaging selects patients that are most likely to benefit from the treatment and predicts the therapeutic impact on the tumour enabling personalised therapy (Drude et al, 2017).

In a previous study, we modified the Sgc8-c aptamer to generate NIR (Near Infrared) and radiolabelled probes (Calzada et al, 2017). Sgc8-c-Alexa647 and Sgc8-c-HYNIC-^{99m}Tc were synthesised and evaluated *in vitro* and *in vivo*. However, in these studies no tumour uptake was observed after injection with radiolabelled probe, although an unspecific signal was shown in the liver and kidneys. The fast clearance and high hydrophilicity of Sgc8-c-HYNIC-^{99m}Tc could account for this biological behaviour. Further structural changes are required to achieve a ^{99m}Tc- probe with higher tumour uptake (Calzada et al, 2017).

Herein, a new modified Sgc8-c aptamer was studied as a new radiolabelled probe. A Sgc8-c 5'-amino derivative was conjugated with DOTA and radiolabelled with ^{67}Ga. The advantage of using Sgc8-c-DOTA is that it can be used as a theranostic probe; the same starting material can be used to prepare diagnostic and therapeutic radiopharmaceuticals by only changing the radionuclide (Calzada et al, 2012). Chelation of Ga^{3+} ions to DOTA is a fast and high-yielding reaction and can be empoyed with other theranostic radionuclides (Drude et al, 2016). There are few studies on aptamers with gallium radionuclides. The labelled aptamer formed by chelation of ^{68}Ga to NOTA was studied by Gijs and co-workers (Gijs et al, 2016). However, ^{67}Ga is a gamma emitting radionuclide ($t_{1/2}$=78hr) and is used to perform imaging over longer periods of time (days) with no cyclotron necessity.

Sgc8-c-DOTA was synthesized with >70% yield using a 200-fold excess of DOTA (Sicco et al, 2017). The Sgc8-c-DOTA intermediate was successfully purified using RP-HPLC. Probe purification process was optimised to obtain high specific activity (Sicco et al, 2017). Radiolabelling with ^{67}Ga resulted in high yields (>95%). Sgc8-c-DOTA-^{67}Ga uptake in A20 and B16F1 cells was significantly higher with respect to positive CCRF-CEM cells in all cases (Figure 3). Binding studies of Sgc8-c-DOTA-^{67}Ga to CCRF-CEM, B16F1 and A20 cell lines showed similar results to those Sgc8-c-probes previously reported (Calzada et al, 2017). Although, serum stability of Sgc8-c-DOTA-^{67}Ga was <50% after 2hr of incubation, the remainder of the probe was sufficient for *in vivo* analyses and to determine pharmacokinetics properties.

Surprisingly, the pharmacokinetic parameters of Sgc8-c-DOTA-^{67}Ga resulted in a high Vss, indicating fast blood clearance and rapid tissue distribution. Biodistributions studies are in agreement with these results, with only 12.99±0.94%ID/g in the blood 30min post IV probe administration and decreasing over 24 hr. No %ID/g value was greater than 15% 30min post probe injection. The third part of the activity was eliminated in the urine. The individual liver values and slowly increasing values over time are consistent with hepatobiliar metabolism. There was poor uptake in bone over time, indicating stable coordination of ^{67}Ga to the Sgc8-c-DOTA probe.

Tumour uptake was analyzed *in vivo* and *ex vivo* imaging. Results were validated in a gamma counter and weight corrected. Preliminary *in vivo* gamma images showed a strong abdominal signal and slight asymmetry on the tumour area. Due to the poor resolution of the images, tumour uptake was confirmed using *ex vivo* imaging. Results indicate that a later time point achieves better tumour uptake. Interestingly, images of both tumour- bearing mouse models showed high hepatobiliar metabolism (followed by quantification in a gamma counter and weight corrected). Tumour:blood and tumour:muscle ratios were >6 and increased over 24hr with probe activity retained in the tumour. This was coupled with greater whole body probe clearance at later time points. No significant kidney uptake was observed and the optimal time points for imaging acquisition were later than expected considering the size and hydrophilicity of the probe.
In summary, the results showed tumour uptake and a hepatobiliar metabolism of the probe. Rate of metabolism could improve tumour uptake but increasing abdominal signal. There are a few previous studies of *in vivo* imaging with radioactive aptamer-derivative probes, showing similar results (Hwang et al, 2010; Gijs et al, 2016). Thus further investigation is needed to acquire a

better understanding of aptamer metabolism and pharmacokinetics as these are key parameters to improve imaging results.

Favourable target:non-target ratios of these aptamer-derivatives highlight their potential as agents for molecular theranostics. Furthermore, due to the enhancement in tumour retention over time, imaging could improve with later time point acquisition. Thus for imaging with ^{67}Ga longer time points, such as 48 and 72hr, may be more suitable.

CONCLUSIONS

The findings reported here present a simple aptamer radiolabelling procedure, as used in the synthesis of Sgc8-c-DOTA-^{67}Ga. Probe injection in tumour melanoma and lymphoma tumour-bearing mice reveals substantial and sustained Sgc8-c-DOTA-^{67}Ga uptake in tumours. In summary, this work highlights the potential of radiolabelled Sgc8-c-DOTA probe in theranostic applications.

ACKNOWLEDGEMENTS

This work was supported by grants from Agencia Nacional de Investigación e Innovación (ANII, Uruguay), PEDECIBA-Química (Uruguay), Comisión Sectorial de Investigación Científica (Universidad de la Republica, Uruguay) and University of Missouri (USA). E. Sicco was funded by a scholarship from the ANII (BE_POS_NAC_2011_1_3493).

COMPETING INTERESTS

None declared.

LIST OF ABBREVIATIONS

AIC: Akaike **I**nformation **C**riteria

CL: Clearance

CLr: renal **C**learance

cpm: counts **p**er **m**inute

Vss: Volume of distribution at **S**teady **S**tate

DOTA: 1,4,7,10-tetraazacyclododecane-1,4,7,10-tetraacetic acid

DMSO: Dimethyl**s**ulf**o**xide

FBS: Fetal **B**ovine **S**erum

HPLC: High **P**erformance **L**iquid **C**hromatography

HYNIC: Hydrazino**nic**otinamide

ID: Injected **D**oses

NIR: Near **I**nfra **R**ed

PBS: Phosphate **B**uffered **S**aline

PTK7: Protein **T**yrosine **K**inase **7**

RP: Reverse **P**hase

SELEX: Systematic **E**volution **L**igands by **EX**ponential Enrichment

REFERENCES

Baum RP, Kulkarni HR and Carreras C. 2012. Peptides and receptors in image-guided therapy: theranostics for neuroendocrine neoplasms. Semin Nucl Med, 42, 190-207.

Berger H, Wodarz A and Borchers A. 2017. PTK7 Faces the Wnt in Development and Disease. Front Cell Dev Biol, 5-31.

Borbas KE, Ferreira CS, Perkins A, Bruce JI and Missailidis S. 2007. Design and synthesis of mono- and multimeric targeted radiopharmaceuticals based on novel cyclen ligands coupled to anti-MUC1 aptamers for the diagnostic imaging and targeted radiotherapy of cancer. Bioconjug Chem, 18, 1205-12.

Breaker RR. 2004. Natural and engineered nucleic acids as tools to explore biology. Nature, 432, 838-845.

Calzada V, Moreno M, Newton J, et al. 2017. Development of new PTK7-targeting aptamer-fluorescent and -radiolabelled probes for evaluation as molecular imaging agents: Lymphoma and melanoma *in vivo* proof of concept. Bioorg Med Chem, 25, 1163-1171.

Calzada V, Zhang X, Fernandez M, et al. 2012. A potencial theranostic agent for EGF-R expression tumors: (177)Lu-DOTA-nimotuzumab. Curr Radiopharm, 5, 318-324.

Cao HY, Yuan AH, Chen W, Shi XS and Miao Y. 2014. A DNA aptamer with high affinity and specificity for molecular recognition and targeting therapy of gastric cancer. BMC Cancer, 14, 699.

Charlton J, Sennello J and Smith D. 1997. *In vivo* imaging of inflammation using an aptamer inhibitor of human neutrophil elastase. Chem Biol, 4, 809-816.

Da Pieve C, Perkins AC and Missailidis S. 2009. Anti-MUC1 aptamers: radiolabelling with (99m)Tc and biodistribution in MCF-7 tumour-bearing mice. Nucl Med Biol. 36, 703-710.

Darmostuk M, Rimpelova S, Gbelcova H and Ruml T. 2015. Current approaches in SELEX: An update to aptamer selection technology. Biotechnol Adv, 33(6 Pt 2), 1141-1161.

Drude N, Tienken L and Mottaghy FM. 2017. Theranostic and nanotheranostic probes in nuclear medicine. Methods, 130, 14-22.

Ellington A and Szostak JW. 1990. In vitro selection of RNA molecules that bind specific ligands. Nature, 346, 818-822.

Gao S, Zheng X, Jiao B and Wang L. 2016. Post-SELEX optimization of aptamers. Anal Bioanal Chem, 408(17), 4567-4573.

García-Recio EM, Pinto-Díez C, Pérez-Morgado MI, et al. 2016. Characterization of MNK1b DNA Aptamers That Inhibit Proliferation in MDA-MB231 Breast Cancer Cells. Mol Ther Nucleic Acids, 5-e275.

Gijs M, Dammicco S, Warnier C, et al. 2016. Gallium-68-labelled NOTA-oligonucleotides: an optimized method for their preparation. J Labelled Comp Radiopharm. 59, 63-71.

Gijs M, Aerts A, Impens N, Baatout S, Luxen A. 2016. Aptamers as radiopharmaceuticals for nuclear imaging and therapy. Nucl Med Biol, 43, 253-271.

Hicke BJ, Stephens AW, Gould T, et al. 2006. Tumor targeting by an aptamer. J Nucl Med, 47, 668-678.

Histed SN, Lindenberg ML, Mena E, Turkbey B, Choyke PL and Kurdziel KA. 2012. Review of functional/anatomical imaging in oncology. Nucl Med Commun, 33, 349-61.

Hwang do W, Ko HY, Lee JH, et al. 2010. A nucleolin-targeted multimodal nanoparticle imaging probe for tracking cancer cells using an aptamer. J Nucl Med, 51, 98-105.

Jacobson O, Weiss ID, Wang L, et al. 2015. 18F-Labeled single-stranded DNA aptamer for PET imaging of protein tyrosine kinase-7 expression. J Nucl Med, 56, 1780-1785.

Kanwar JR, Roy K, Maremanda NG, et al. 2015. Nucleic acid-based aptamers: applications, development and clinical trials. Curr Med Chem, 22, 2539-2557.

Lee DY and Li KC. 2011. Molecular theranostics: a primer for the imaging professional. AJR Am J Roentgenol, 197, 318-324.

Lindmo T and Bunn PA Jr. 1986. Determination of the true immunoreactive fraction of monoclonal antibodies after radiolabeling. Methods Enzymol, 121, 678-691.

Nozari A, Berezovski MV. 2017. Aptamers for CD Antigens: From Cell Profiling to Activity Modulation. Mol Ther Nucleic Acids, 6, 29-44.

Osborne SE and Ellington AD. 1997. Nucleic Acid Selection and the Challenge of Combinatorial Chemistry. Chem Rev, 97, 349-370.

Palestro CJ. 2014. Nuclear medicine and the failed joint replacement: Past, present, and future. World J Radiol, 6, 446-458.

Parashar A. 2016. Aptamers in therapeutics. J Clin Diagn Res, 10, BE01-6.

Röthlisberger P, Gasse C, Hollenstein M. 2017. Nucleic acid aptamers: Emerging applications in medical imaging, nanotechnology, neurosciences, and drug delivery. Int J Mol Sci, 18, Pii: E2430.

Shangguan D, Li Y, Tang Z, et al. 2006. Aptamers evolved from live cells as effective molecular probes for cancer study. Proc Natl Acad Sci U S A, 103, 11838-11843.

Shangguan D, Tang Z, Mallikaratchy P, Xiao Z and Tan W. 2007. Optimization and modifications of aptamers selected from live cancer cell lines. Chembiochem, 8, 603-606.

Shangguan D, Cao Z, Meng L, et al. 2008. J Cell-specific aptamer probes for membrane protein elucidation in cancer cells. Proteome Res, 7, 2133-2139.

Sicco E, Baez J, Margenat J, et al. 2017. Derivatizations of Sgc8-c aptamer to prepare metallic radiopharmaceuticals as imaging diagnostic agents: Syntheses, isolations, and physicochemical characterizations. Chem Biol Drug Des, doi: 10.1111/cbdd.13135.

Stein CA and Castanotto D. 2017. FDA-Approved Oligonucleotide Therapies in 2017. Mol Ther, 25, 1069-1075.

Sun H, Zhu X, Lu PY, Rosato RR, Tan W and Zu Y. 2014. Oligonucleotide aptamers: new tools for targeted cancer therapy. Mol Ther Nucleic Acids, 3, e182.

Tuerk C and Gold L. 1990. Systematic evolution of ligands by exponential enrichment: ARN ligands to bacteriophage T4 DNA polymerase. Science, 249, 505-510.

Weissleder R and Mahmood U. 2001. Molecular imaging. Radiology, 219, 316-333.

Wu YX and Kwon YJ. 2016. Aptamers: The "evolution" of SELEX. Methods, 106, 21-28.

Xiao Z, Shangguan D, Cao Z, Fang X, Tan W. 2008. Cell-specific internalization study of an aptamer from whole cell selection. Chemistry - A European Journal, 1769-1775.

Wang AZ and Farokhzad OC. 2014. Current progress of aptamer-based molecular imaging. J Nucl Med, 55, 353-356.

FIGURES:

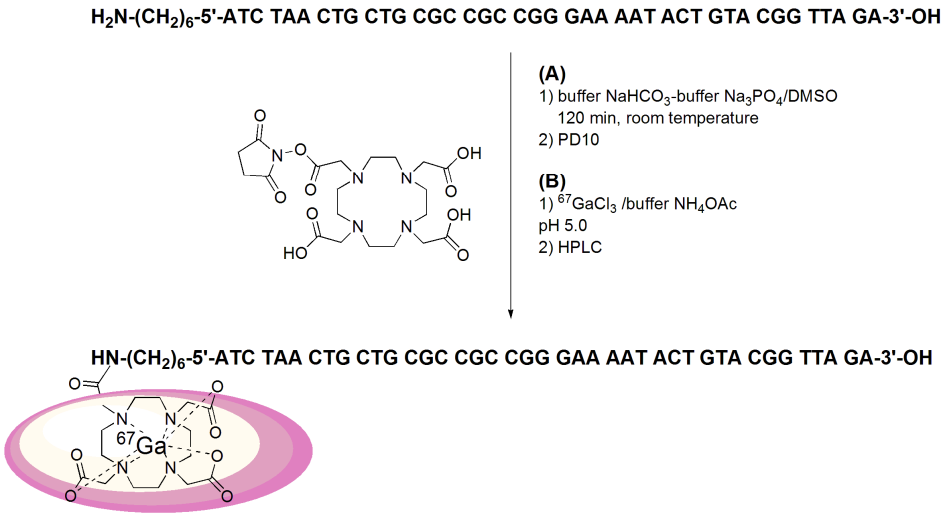

Figure 1. Schematic procedure for the preparation of Sgc8-c-DOTA and Sgc8-c-DOTA-^{67}Ga. Sgc8-c-NH_2 reaction with NHS-DOTA (A) and radiolabelling with ^{67}Ga (B).

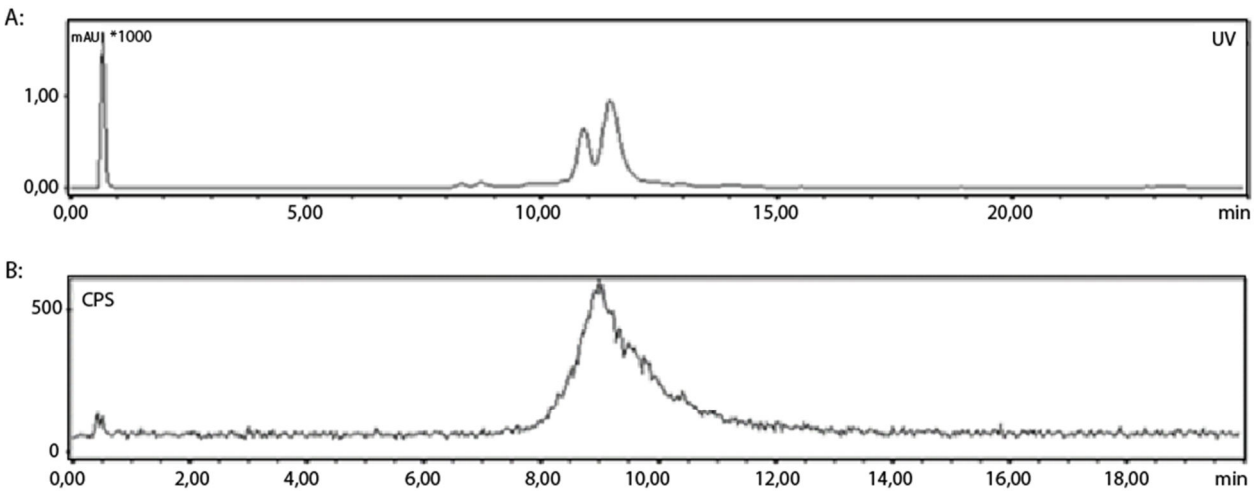

Figure 2. RP-HPLC profiles of the Sgc8-c-DOTA intermediate reaction mixture and Sgc8-c-DOTA-^{67}Ga. **A.** The UV trace of the reaction mixture containing Sgc8-c-NH_2 (first peak; 10.8min) and Sgc8-c-DOTA (second peak, 11.5min). **B.** A gamma detection chromatograph of the Sgc8-c-DOTA-^{67}Ga. [mAU = milli-**Absorbance** Units; *1000 = 1000 x mAU]

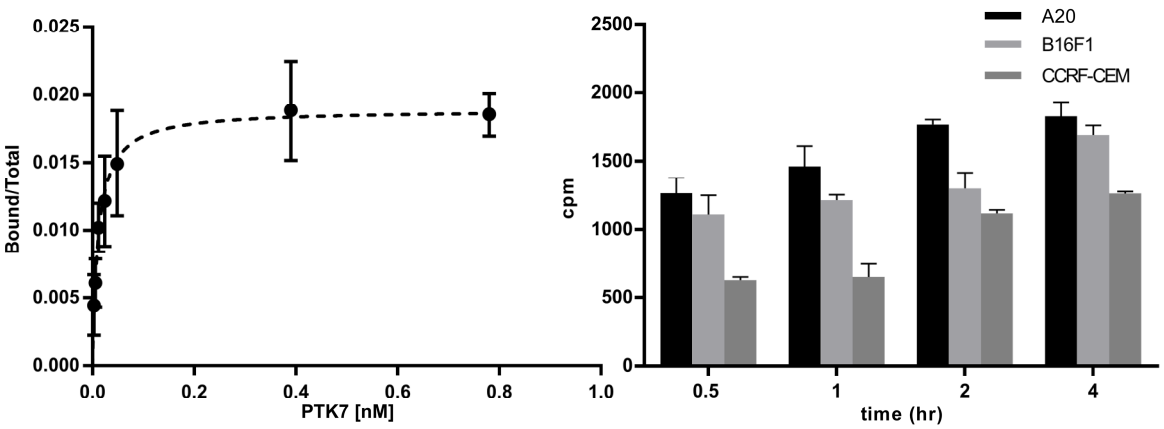

Figure 3. Maximum binding capacity assay performed with Sgc8-c-DOTA-^{67}Ga (left). Binding of Sgc8-c-DOTA-^{67}Ga to A20 and B16F1 cell lines. Positive control: CCRF-CEM (Shangguang et al, 2008). At each time binding data from both cell lines was significantly different respect to positive control (right).

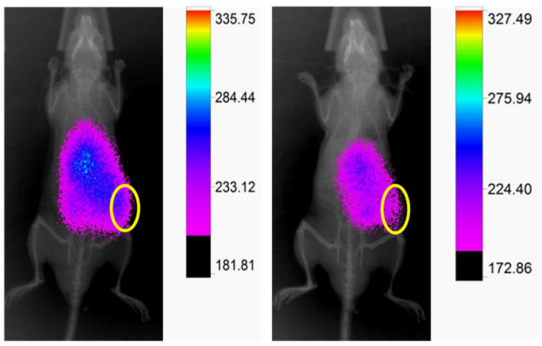

Figure 4. *In vivo* images at 2hr (left) and 24hr (right) post injection of Sgc8-c-DOTA-^{67}Ga in B16F1-tumour bearing C57BL/6-mice. Tumour location is highlighted by the yellow oval.

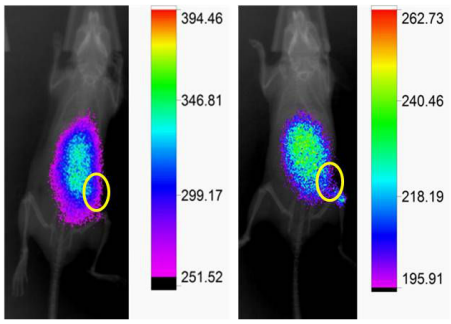

Figure 5. *In vivo* images at 2hr (left) and 24hr (right) post injection of Sgc8-c-DOTA-^{67}Ga in A20-tumour bearing BALB/c mice. The tumour location is highlighted by the yellow oval.

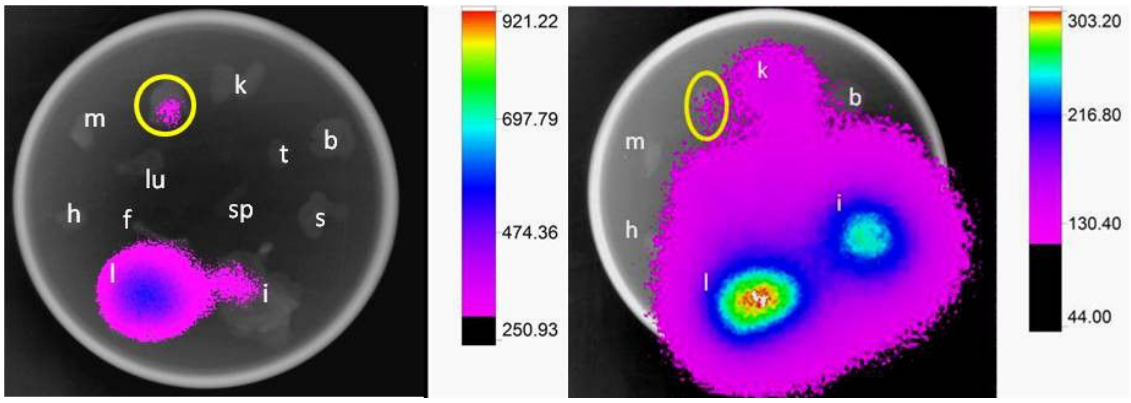

Figure 6. *Ex vivo* images of organs and tissues 24hr after injection with Sgc8-c-DOTA-^{67}Ga to melanoma (left) and lymphoma (right) tumour bearing mice. Yellow circles show the tumour location, brain (b), femour (f), heart (h), intestines (i), kidneys (k), liver (l), lung (lu), muscle (m), stomach (s), spleen (sp), thyroid (t) are presented.

Table 1. Biodistribution results for Sgc8-c-DOTA-^{67}Ga at 0.5, 2, 4 and 24 hr post injection in BALB/c normal mice.

Organ/ Tissue		Time		
	0.5 hr	**2 hr**	**4hr**	**24 hr**
	Percentage of injected doses per organ weight (%ID/g ± sd)			
Blood	12.99 ± 0.94	13.51 ± 2.03	11.93 ± 2.39	3.55 ± 1.79
Liver	12.38 ± 1.75	14.12 ± 1.35	13.12 ± 2.21	13.19 ± 3.10
Heart	4.16 ± 1.40	4.78 ± 1.35	3.31 ± 0.56	2.20 ± 1.01
Lungs	11.23 ± 1.09	18.00 ± 1.50	13.34 ± 5.67	10.34 ± 2.49
Spleen	4.53 ± 0.81	7.21 ± 1.56	5.32 ± 3.34	11.06 ± 2.91
Kidneys	5.48 ± 0.80	7.64 ± 0.62	7.50 ± 1.17	8.65 ± 1.38
Thyroid	6.91 ± 0.91	5.13 ± 3.33	4.63 ± 1.26	1.64 ± 1.39
Muscle	1.83 ± 0.44	1.48 ± 0.39	1.59 ± 0.84	0.57 ± 0.33
Bone	4.25 ± 0.62	7.22 ± 4.11	6.98 ± 0.93	10.84 ± 1.55
Stomach	1.71 ± 0.03	2.66 ± 0.53	2.17 ± 0.88	2.40 ± 0.49
Intestine	3.08 ± 0.25	4.47 ± 0.99	5.69 ± 1.04	9.97 ± 1.41
Brain	0.39 ± 0.13	0.82 ± 0.51	0.50 ± 0.43	0.30 ± 0.16
	Percentage of injected doses (%ID ± sd)			
Urine + Bladder	8.17 ± 0.48	5.17 ± 2.05	14.99 ± 3.51	31.23 ± 1.90